Two Component Dark Matter : A Possible Explanation of 130 GeV $\gamma-$Ray Line from the Galactic Centre

Anirban Biswas† [1], **Debasish Majumdar**† [2], **Arunansu Sil**‡ [3], **Pijushpani Bhattacharjee**† [4]

† *Astroparticle Physics and Cosmology Division, Saha Institute of Nuclear Physics, Kolkata 700064, India*

‡ *Department of Physics, Indian Institute of Technology, Guwahati, Guwahati 781039, India*

ABSTRACT

Recently there has been a hint of a gamma-ray line at 130 GeV originated from the galactic centre after the analysis of the Fermi-LAT satellite data. Being monochromatic in nature, it rules out the possibility of having its astrophysical origin, and there has been a speculation that this line could be originated from dark matter annihilation. In this work, we propose a two component dark matter scenario where an extension of the Standard model by an inert Higgs doublet and a gauge singlet scalar concocted with $Z_2 \times Z'_2$ symmetry, is considered. We find that our scenario can not only explain the 130 GeV gamma-ray line through dark matter annihilation but also produce the correct dark matter relic density. We have used the Standard Model Higgs mass around 125 GeV as intimated by the LHC data.

[1] email: anirban.biswas@saha.ac.in
[2] email: debasish.majumdar@saha.ac.in
[3] email: sil.arunansu@gmail.com
[4] email: pijush.bhattacharjee@saha.ac.in

1 Introduction

Although the existence of dark matter (DM) is now established by various astronomical measurements and observations where the gravitational effects of this huge amount of dark matter is manifested, the particle nature of the dark matter still remains unknown. The particle nature of the dark matter can be probed if it is detected either by direct detection process or by indirect detection. In the former the energy of recoil of a detector nucleus is to be measured if a dark matter indeed scatters off such a nucleus or nucleon. On the other hand the dark matter can be gravitationally trapped inside massive celestial objects such as sun, in regions of galactic centre etc. These trapped dark matter particles eventually annihilate to produce fermion-antifermion pairs or γs. Study of dark matter through the indirect detection whereby such annihilation products are detected and analyzed, may reveal the nature of the dark matter. Recently much interest is generated by the evidence of monochromatic 130 GeV γ-rays from the direction of galactic centre obtained from the analysis [1, 2] of observational data [3] from the Fermi-LAT satellite borne telescope. This phenomenon could not be explained due to other astrophysical events and the observance of γ-ray, is strongly suggestive of being produced by the annihilation of dark matter at the Galactic centre region.

In the present work we propose a particle physics model for dark matter that can explain the 130 GeV γ-line observed by Fermi-LAT. Our model is in fact a two-component dark matter model in which a real scalar singlet and an inert doublet are added to the Standard Model (SM) of particle physics. There are previous works where either the real scalar singlet model or the inert doublet model has been discussed as one component dark matter model. But, as it will be revealed later that any one of these two models fail to explain individually (as one component dark matter) the observed 130 GeV γ-line from the galactic centre if it is produced due to dark matter annihilation.

In earlier works such as Ref.[4], the authors showed that the scalar dark matter can annihilate into $\gamma\gamma$ final state with the help of additional charged scalars in a model independent way. It would yield 130 GeV γs with the required annihilation cross section ($\langle\sigma \mathrm{v}_{\gamma\gamma}\rangle \sim 10^{-27}\mathrm{cm}^3/\mathrm{s}$ given by the analysis [1] of the Fermi-LAT data mentioned above). Different other possibilities involving new particles originated from different extensions of SM have been investigated [5, 6] to explain the 130 GeV γ-line through DM (single candidate) annihilation. However most of these endeavours are restricted in obtaining $\langle\sigma \mathrm{v}_{\gamma\gamma}\rangle \sim 10^{-27}\mathrm{cm}^3/\mathrm{s}$ without going into detailed discussions on relic density calculations, calculation of scattering cross sections relevant for direct detection and their comparisons with experimental (direct detection experiments) or observational (WMAP [7]) results.

One of the simplest choice to accommodate a dark matter is to extend the SM with a gauge

singlet real scalar field S (we will call it real scalar singlet dark matter model, RSDM, from now on) [8, 9, 10], which couples to SM Higgs (h). The use of a Z_2 symmetry ensures the stability of the dark matter candidate. In ref.[10] it is shown that this type of model fails to explain the 130 GeV gamma-ray line from the Galactic centre. The reason of this failure is related with the relatively small annihilation cross section of two S fields into two γs considering the fact that S should contribute to the correct amount of relic density as predicted by WMAP data [7]. In [9], it was shown that with SM Higgs much heavier than 125 GeV could in principle lead to $\langle \sigma \mathrm{v}_{\gamma\gamma} \rangle \sim 10^{-27}\mathrm{cm}^3/\mathrm{s}$ with $m_S \sim 130$ GeV, when the constraint on the S field to produce right amount of dark matter abundance is relaxed. However once this constraint is applied, the $\langle \sigma \mathrm{v}_{\gamma\gamma} \rangle$ becomes few orders of magnitude less than required. In addition to these findings, if we employ the recent constraint on the Higgs mass from LHC experiment [11] on the SM Higgs, then we infer that strictly within RSDM picture, we can not accommodate both the relic density as well as the 130 GeV γ-line from DM annihilation.

Another well motivated dark matter model is the inert doublet model (IDM) [12, 13, 14] which requires an extension of the SM by a scalar Higgs (inert) doublet Φ having a Z_2. In ref.[13], it was shown that there exists an allowed region (consistent with the WMAP results of relic density) in IDM for dark matter[5] ϕ^0 having mass in the range between 80 GeV and 160 GeV provided the mass of the dark matter candidate (m_{ϕ^0}) is less than the mass of SM Higgs (and top quark), $m_{\phi^0} < m_{h,t}$. This condition was imposed to reduce the $\langle \sigma \mathrm{v} \rangle_{\mathrm{total}}$ (to get rid of the contributions like $\phi^0\phi^0 \to hh$ (and/or tt)) since otherwise the relic density would be small[6]. Then they found that due to accidental cancellations of different Feynman diagrams for annihilation into gauge bosons, $\langle \sigma \mathrm{v} \rangle_{\mathrm{total}}$ can indeed be the right amount for a judicious choice of parameter space involved in the model.

We are trying to find a resolution where a right amount of dark matter relic density could be obtained as well as an explanation of the 130 GeV gamma-ray line of Fermi-LAT can also be probed through DM annihilation. Now with the consideration that the SM Higgs boson has a mass $m_h \sim 125$ GeV [11] and mass of the DM candidate 130 GeV (in order to explain the 130 GeV gamma-ray line from Fermi-LAT, the mass of the DM should be in this range), the above mentioned condition $m_{\phi^0} < m_{h,t}$ related to the IDM is evaded thereby the channel of annihilation, $\phi^0\phi^0 \to hh$, opens up. Hence $\langle \sigma \mathrm{v} \rangle_{total}$ will increase and the final relic density in this sort of model can accommodate only (10-30)% of the observed DM relic density [13]. However this result has an interesting consequence. We can compensate this deficit of the DM relic density by another candidate of DM while ϕ^0 explains the 130 GeV gamma-line through its annihilation.

Keeping in mind the above mentioned scenarios (particularly the RSDM and IDM), we pro-

[5] ϕ^0 is the neutral component of the extra Higgs doublet.
[6] since relic density $\Omega h^2 \propto 1/\langle \sigma \mathrm{v} \rangle$.

pose that the dark matter can actually be composed of two fields, namely a scalar singlet (S) and an inert doublet (Φ). The additional feature of this model would be that these two components possess an interaction between them via a term like $(\Phi^\dagger\Phi)SS$. The 130 GeV γ-line will be produced by the annihilation of the component ϕ^0 while the role of other component S, besides contributing to the overall relic density is to increase ϕ^0 contribution to the combined relic density through $(\Phi^\dagger\Phi)SS$. A model with a scalar singlet and a doublet was presented in [15] in the context of GUT models. A multi-component dark matter was proposed in [16] earlier where an additional fermion singlet and a scalar singlet were introduced, though not in the context of the possibility of having 130 GeV gamma-ray from DM annihilation. We have imposed a discrete $\mathrm{Z}_2 \times \mathrm{Z}_2'$, under which S and Φ transform non-trivially.

The calculation of the flux for 130 GeV γ-ray from galactic centre region also requires the knowledge of dark matter density in the region of the galactic centre. In the absence of a unique density profile in literature we consider in the present work two dark matter density profiles namely NFW (Navarro-Frenk-White) profile [17] and Einasto profile [18] and compute the flux using the cross section $\langle \sigma \mathrm{v}_{\phi^0\phi^0\to\gamma\gamma}\rangle$ calculated in this work from our model.

The paper is arranged as follows. In Section 2 we describe the structure of our two component dark matter model. Section 3 discusses the calculations of the relic densities of each dark matter components and hence the combined relic density by simultaneously solving the two Boltzmann's equations for the two components. In Section 4 we discuss how to constrain the parameter space of the model by comparing the relic density results with WMAP and the scattering cross section results with the direct detection experiments data. Section 5 gives the cross section calculations for 130 GeV γ-ray from $\phi^0\phi^0$ annihilation and hence the calculations of γ-ray flux using different dark matter halo models. Finally in Section 6 we present some discussions and conclusions.

2 The Two Component Dark Matter Model

In the present work, the DM sector is composed of a real gauge singlet scalar field, S and an extra (in addition to the usual Higgs doublet, H) scalar doublet field, Φ (doublet under $SU(2)_{\mathrm{L}}$). An exact (unbroken) discrete symmetry $\mathrm{Z}_2 \times \mathrm{Z}_2'$ is imposed under which all the SM particles are even, i.e. having $\mathrm{Z}_2 \times \mathrm{Z}_2'$ charge as (1,1) and for Φ, S the $\mathrm{Z}_2 \times \mathrm{Z}_2'$ charges are (1,-1) and (-1,1) respectively. Thereby both S and Φ are fermiophobic and do not develop any vacuum expectation value (VEV) and hence inert. The construction therefore ensures the stability of both S and Φ in this two component dark matter scenario. The scalar doublet Φ can be written

as

$$\Phi = \begin{pmatrix} \phi^+ \\ \frac{\phi^0 + iA^0}{\sqrt{2}} \end{pmatrix} . \tag{1}$$

The Lagrangian of the construction can be read as, $\mathcal{L} = \mathcal{L}_{\rm SM} + \mathcal{L}_{\rm DM}$, where $\mathcal{L}_{\rm SM}$ is the Standard Model Lagrangian and $\mathcal{L}_{\rm DM}$ stands for the DM sector consistent with all the symmetries. $\mathcal{L}_{\rm DM}$ is then given by,

$$\mathcal{L}_{\rm DM} = \mathcal{L}_{\rm RSDM} + \mathcal{L}_{\rm IDM} + \mathcal{L}_{\rm INT}, \tag{2}$$

where $\mathcal{L}_{\rm RSDM}$ and $\mathcal{L}_{\rm IDM}$ refer to the individual Lagrangian of real singlet scalar and inert doublet dark matter respectively and $\mathcal{L}_{\rm INT}$ is the additional part representing the interaction between the two components of DM. So the most general form of them, consistent with the SM gauge group as well as the discrete symmetry imposed, is as follows,

$$\begin{aligned}
\mathcal{L}_{\rm RSDM} &= \frac{1}{2}\partial_\mu S \partial^\mu S - \frac{\kappa_1^2}{2}S^2 - \frac{\kappa_2}{4}S^4 - \lambda_6({\rm H}^\dagger {\rm H})SS, && (3)\\
\mathcal{L}_{\rm IDM} &= (D_\mu\Phi)^\dagger(D^\mu\Phi) - \mu_2^2(\Phi^\dagger\Phi) - \rho_2(\Phi^\dagger\Phi)^2 - \lambda_1({\rm H}^\dagger{\rm H})(\Phi^\dagger\Phi) - \\
&\quad \lambda_2(\Phi^\dagger{\rm H})({\rm H}^\dagger\Phi) - \lambda_3\left[(\Phi^\dagger{\rm H})^2 + h.c\right], && (4)\\
\mathcal{L}_{\rm INT} &= -\lambda_5\left(\Phi^\dagger\Phi\right)SS. && (5)
\end{aligned}$$

The SM Higgs Lagrangian is included in the $\mathcal{L}_{\rm SM}$. In this model we have five new particles, two charged scalar ($\phi^\pm$) and three neutral scalar particles (ϕ^0, S, A^0). Due to the stability and electrical charge neutrality we consider ϕ^0 and S as two viable components of dark matter in this model.

After spontaneous breaking of the SM gauge symmetry, the masses of these new particles and Higgs are given by,

$$\begin{aligned}
m^2_{\phi^\pm} &= \mu_2^2 + \frac{1}{2}\lambda_1 v^2, && (6)\\
m^2_{\phi^0} &= \mu_2^2 + \alpha v^2, && (7)\\
m^2_{A^0} &= \mu_2^2 + \beta v^2, && (8)\\
m^2_S &= \kappa_1^2 + \lambda_6 v^2, && (9)\\
m^2_h &= 2\rho_1 v^2, && (10)
\end{aligned}$$

where v (= 246 GeV) is the Higgs VEV and ρ_1 ($= \sqrt{\frac{m_h^2}{2v^2}}$) is the coefficient of the quartic coupling of the SM Higgs (part of $\mathcal{L}_{\rm SM}$ here) potential. The parameters α and β are defined in terms of λ's as

$$\begin{aligned}
\alpha &= \frac{1}{2}(\lambda_1 + \lambda_2 + 2\lambda_3), \\
\beta &= \frac{1}{2}(\lambda_1 + \lambda_2 - 2\lambda_3). && (11)
\end{aligned}$$

As is evident from the above set up, the model involves 10 parameters in total, specifically m_h, m_{ϕ^0}, m_{A^0}, m_{ϕ^+}, m_S, α, λ_5, λ_6, κ_2, ρ_2. Now fixing the Higgs mass m_h at 125 GeV, we have altogether 9 parameters, which are further restricted from theoretical bounds as well as from experimental results as discussed below.

- **Vacuum Stability** - The Lagrangian of this model (Eq. (2)) must be bounded from below. This condition will be satisfied if

$$
\begin{aligned}
\rho_1,\, \rho_2,\, \kappa_2 &> 0\,, && (12)\\
\alpha, \beta &> -\sqrt{\rho_1\rho_2}\,, && (13)\\
\lambda_1 &> -2\sqrt{\rho_1\rho_2}\,, && (14)\\
\lambda_6 &> -2\sqrt{\rho_1\kappa_2}\,, && (15)\\
\lambda_5 &> 2\sqrt{\rho_2\kappa_2}\,. && (16)
\end{aligned}
$$

- **Zero VEV of Φ and S** - Ground state of the Lagrangian Eq. (2) must preserve $Z_2 \times Z_2'$ symmetry for stability of the dark matter candidates, this leads to the condition that the VEV of both Φ, S is zero.

- **Perturbativity**- In order to be within the perturbative limit, the model parameters cannot be too large. This can be ensured provided

$$|\text{model parameters}| < 4\pi. \tag{17}$$

- **Neutral Scalar Mass** - The LEP [19] measurement of the Z boson decay width leads to the condition

$$m_{A^0} + m_{\phi^0} > m_Z. \tag{18}$$

- **WMAP Limit** - The Combined relic density of the dark matter components must satisfy the WMAP limit [7],

$$0.1053 < \Omega_{\rm DM}h^2 < 0.1165 \;\; \text{at} \;\; 68\% \;\; \text{C.L.} \tag{19}$$

  for the dark matter in the Universe. This condition will further constrain the parameter space of this model discussed above.

- **Direct detection limits of dark matter** - The results of the ongoing experiments for direct detection of dark matter also impose additional limits on the relevant parameters of the present two component dark matter model. Being inert, the elastic scattering between

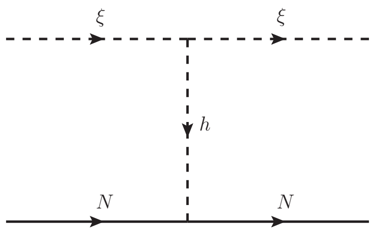

Figure 1: Feynman diagram for the elastic scattering between dark matter particle ξ (i,e. S, ϕ^0) and nucleon N of the detector material via Higgs exchange.

the dark matter candidate ξ (here ϕ^0 and/or S) and nucleons (N) can take place only with the SM Higgs exchange as in Fig 1. The relevant term in the Lagrangian which describes the interaction between ξ and Higgs is given by

$$\mathcal{L} = -k\xi^2 h, \tag{20}$$

where the coupling $k = \alpha v$ ($\lambda_6 v$) for $\xi = \phi^0$ (S). The spin independent scattering cross section for this process, $\xi N \to \xi N$, is given by[20],

$$\sigma^{\rm SI} = \frac{f^2}{\pi}\left(\frac{k}{v}\right)^2 \frac{\mu^2\, m_N^2}{m_\xi^2\, m_h^4}\,, \tag{21}$$

where m_ξ and m_N are the masses of the DM candidate and nucleons respectively, $\mu = \frac{m_\xi m_N}{m_\xi + m_N}$ is the reduced mass and f represents the strength of the effective interaction which depends upon the number of heavy quarks involved [21]. In this work, we have considered the value of $f = 0.3$ [14, 22].

An upper limit on $\sigma^{\rm SI}$ for a particular mass of dark matter particle would automatically sets an upper bound on the absolute value of the couplings α and λ_6. Since our goal is to explain the 130 GeV γ-ray line from annihilation of one of the DM candidates in the present two component dark matter model, that particular component should have a mass near 130 GeV. The upper limit on $\sigma^{\rm SI}$ for a 130 GeV DM candidate as obtained from XENON 100 (2012) [23] data, is $\sim 3 \times 10^{-45}$ cm^2 at 90% C.L., which in turn specifies the range of α and λ_6 as

$$|\alpha|\,,\, |\lambda_6| \leq 0.038\,, \tag{22}$$

The similar ranges for α, λ_6 from XENON 100 (2011) [24] data are obtained as

$$|\alpha|\,,\, |\lambda_6| \leq 0.076\,. \tag{23}$$

The result obtained from XENON 100 (2011) data was less constrained than 2012 data. This will be discussed in Section 4 while constraining the parameter space. Upper limits set by XENON 100 (2012) on $\sigma^{\rm SI}$ with respect to dark matter mass lie below the similar limits obtained from other recent ongoing dark matter direct detection experiments such as CDMS-II [25], EDELWEISS-II [26] etc. Therefore the limit given in Eq. (22) for a 130 GeV dark matter particle must also satisfy the limits (from ($\sigma^{\rm SI} - m_\chi$) exclusion plots) obtained from other direct detection experiments .

3 Combined Relic Density Calculation for the two dark matter Candidates ϕ^0 and S

In the present two component dark matter model, the total relic density of the dark matter in the universe will have contributions from both the components S and ϕ^0. While both are annihilating into the SM particles, the heavier component, S can annihilate into the lighter component, ϕ^0 too. In order to obtain the correct combined relic density we have to solve Boltzmann's equation for each components simultaneously. The coupled Boltzmann's equations [27] to study the evolution of the number densities of the two dark matter candidates (n_S and n_{ϕ^0}) are given by,

$$\frac{dn_S}{dt} + 3n_S H = -\langle \sigma {\rm v}_{SS\rightarrow\chi\bar\chi}\rangle \left(n_S^2 - (n_S^{eq})^2\right) - \langle \sigma {\rm v}_{SS\rightarrow\phi^0\phi^0}\rangle \left(n_S^2 - \frac{(n_S^{eq})^2}{(n_{\phi^0}^{eq})^2} n_{\phi^0}^2\right) , \tag{24}$$

$$\frac{dn_{\phi^0}}{dt} + 3n_{\phi^0} H = -\langle \sigma {\rm v}_{\phi^0\phi^0\rightarrow\chi\bar\chi}\rangle \left(n_{\phi^0}^2 - (n_{\phi^0}^{eq})^2\right) + \langle \sigma {\rm v}_{SS\rightarrow\phi^0\phi^0}\rangle \left(n_S^2 - \frac{(n_S^{eq})^2}{(n_{\phi^0}^{eq})^2} n_{\phi^0}^2\right) . \tag{25}$$

Here $n_{\phi^0}^{eq}$ and n_S^{eq} are the equilibrium values of n_{ϕ^0} and n_S respectively, H is the Hubble's constant. χ represents any SM particle such as leptons, quarks, gauge bosons, Higgs boson. The annihilation of SS into $\phi^0\phi^0$ is included through the annihilation cross section $\langle \sigma {\rm v}_{SS\rightarrow\phi^0\phi^0}\rangle$, the expression of which in our scenario is discussed later in this section explicitly along with the total annihilation cross section.

Introducing two dimensionless variables $Y_i = \frac{n_i}{s}$ and $x_i = \frac{m_i}{T}$ with $i = S, \phi^0$, where s and T are the entropy density and temperature of the universe respectively, Eqs. (24, 25) can be written as

$$\frac{dY_S}{dx_S} = -\left(\frac{45G}{\pi}\right)^{-\frac{1}{2}} \frac{m_S}{x_S^2}\sqrt{g_\star} \left(\langle \sigma {\rm v}_{SS\rightarrow\chi\bar\chi}\rangle \left(Y_S^2 - (Y_S^{eq})^2\right) + \langle \sigma {\rm v}_{SS\rightarrow\phi^0\phi^0}\rangle \left(Y_S^2 - \frac{(Y_S^{eq})^2}{(Y_{\phi^0}^{eq})^2} Y_{\phi^0}^2\right)\right) , \tag{26}$$

$$\frac{dY_{\phi^0}}{dx_{\phi^0}} = -\left(\frac{45G}{\pi}\right)^{-\frac{1}{2}} \frac{m_{\phi^0}}{x_{\phi^0}^2}\sqrt{g_\star}\left(\langle\sigma \mathrm{v}_{\phi^0\phi^0\to\chi\bar{\chi}}\rangle\left(Y_{\phi^0}^2-(Y_{\phi^0}^{eq})^2\right)-\langle\sigma \mathrm{v}_{SS\to\phi^0\phi^0}\rangle\left(Y_S^2-\frac{(Y_S^{eq})^2}{(Y_{\phi^0}^{eq})^2}Y_{\phi^0}^2\right)\right) . \tag{27}$$

Here G is the Gravitation constant, and $g_\star$ is defined as,

$$\sqrt{g_\star} = \frac{h_{\text{eff}}(T)}{\sqrt{g_{\text{eff}}(T)}}\left(1+\frac{1}{3}\frac{d\ln(h_{\text{eff}}(T))}{d\ln(T)}\right) , \tag{28}$$

with $g_{\text{eff}}(T)$ and $h_{\text{eff}}(T)$ are the effective degrees of freedom related to the energy and entropy densities through $\rho = g_{\text{eff}}(T)\frac{\pi^2}{30}T^4$, $s = h_{\text{eff}}(T)\frac{2\pi^2}{45}T^3$.

Once we get the values of Y_{ϕ^0} and Y_S at the present temperature T_0 after solving the coupled Eqs. (26, 27), we will be able to calculate the individual contributions Ω_{ϕ^0} and Ω_S from [28],

$$\Omega_i h^2 = 2.755\times 10^8\left(\frac{m_i}{\text{GeV}}\right)Y_i(T_0) , \tag{29}$$

(using the present values of s and h). In this work we have solved the coupled Boltzmann equations numerically to get the values of $Y_i(T_0)$. After having these estimates, the total relic density of the universe can be obtained through

$$\Omega_c h^2 = \Omega_{\phi^0}h^2 + \Omega_S h^2 . \tag{30}$$

As we mentioned before, $\langle\sigma \mathrm{v}_{SS\to\chi\bar{\chi}}\rangle$ in Eq.(24) represents the total annihilation cross section of two S particles into SM particles such as leptons and quarks ($f\bar{f}$), gauge bosons (W^+W^-, ZZ) and Higgs boson (h). The Feynman diagrams for all the processes are shown in Fig. 2. The expressions of annihilation cross sections of two S particles for these final states are given below [29].

$$\langle\sigma \mathrm{v}_{SS\to f\bar{f}}\rangle = \left(\frac{g_{SSh}}{v}\right)^2\frac{m_f^2}{\pi}\frac{\left(1-\frac{m_f^2}{m_S^2}\right)^{3/2}}{[(4m_S^2-m_h^2)^2+(\Gamma_h m_h)^2]} , \tag{31}$$

$$\langle\sigma \mathrm{v}_{SS\to W^+W^-}\rangle = 2\left(\frac{g_{SSh}}{v}\right)^2\frac{m_S^2}{\pi}\frac{\left(1-\frac{m_W^2}{m_S^2}\right)^{1/2}}{[(4m_S^2-m_h^2)^2+(\Gamma_h m_h)^2]}\left(1-\frac{m_W^2}{m_S^2}+\frac{3}{4}\frac{m_W^4}{m_S^4}\right) , \tag{32}$$

$$\langle\sigma \mathrm{v}_{SS\to ZZ}\rangle = \left(\frac{g_{SSh}}{v}\right)^2\frac{m_S^2}{\pi}\frac{\left(1-\frac{m_Z^2}{m_S^2}\right)^{1/2}}{[(4m_S^2-m_h^2)^2+(\Gamma_h m_h)^2]}\left(1-\frac{m_Z^2}{m_S^2}+\frac{3}{4}\frac{m_Z^4}{m_S^4}\right) , \tag{33}$$

$$\begin{aligned}\langle\sigma \mathrm{v}_{SS\to hh}\rangle = {} & \frac{1}{4\pi m_S^2}\left(1-\frac{m_h^2}{m_S^2}\right)^{1/2}\Bigg[\left(\frac{3\,g_{SSh}\,m_h^2}{2v(4m_S^2-m_h^2)}\right)^2+g_{SShh}^2+\frac{3\,g_{SSh}\,g_{SShh}\,m_h^2}{v(4m_S^2-m_h^2)} \\ & +\left(\frac{2\,g_{SSh}^2}{2m_S^2-m_h^2}\right)^2+\frac{4\,g_{SSh}^2 g_{SShh}}{2m_S^2-m_h^2}+\frac{6\,g_{SSh}^3 m_h^2}{v(2m_S^2-m_h^2)(4m_S^2-m_h^2)}\Bigg] .\end{aligned} \tag{34}$$

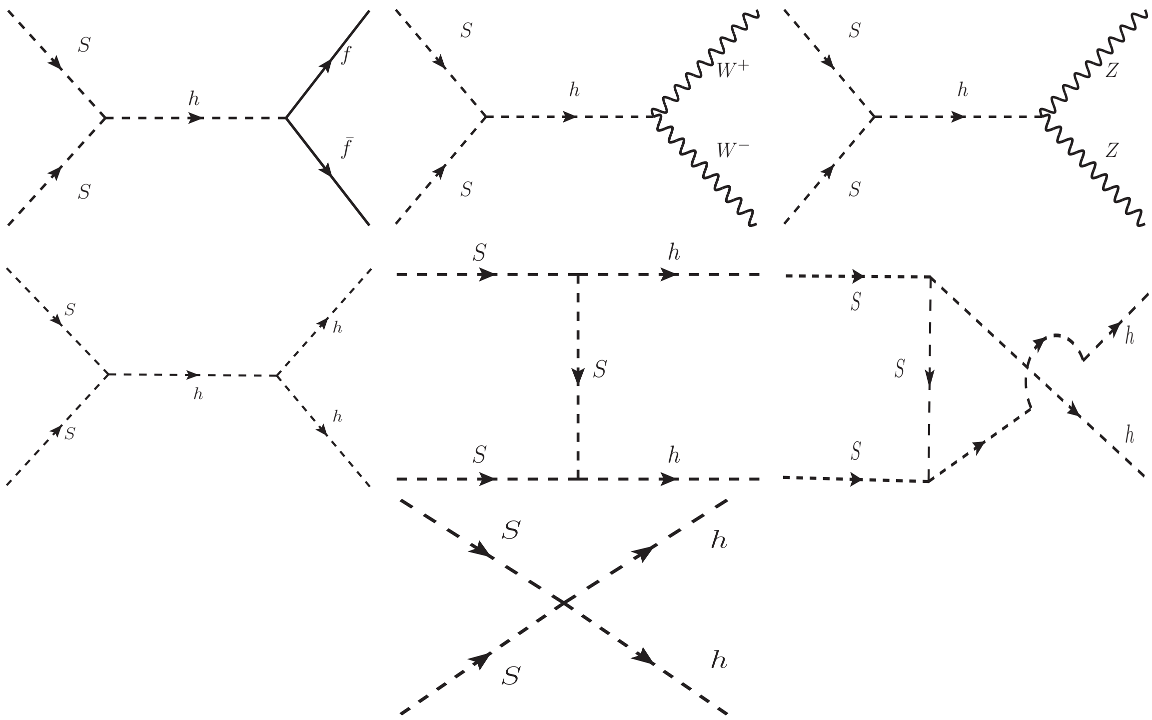

Figure 2: Lowest order Feynman diagrams of two S annihilate into a pair of fermion and anti-fermion, W^+W^-, ZZ and Higgs.

In writing the expression for the cross sections, we have introduced the notation g_{xyz} (or g_{xyzp}) which are related to the coupling constants of the corresponding interaction Lagrangian through $\mathcal{L} = g_{xyz}XYZ$ (or $\mathcal{L} = g_{xyzp}XYZP$). Here X, Y, Z, P are the fields involved in a particular process. All the g_{XYZ} and g_{XYZP} are listed in Table 1. The masses for fermion f, W boson, Z boson and Higgs boson are denoted by m_f, m_W, m_Z, m_h respectively and Γ_h represents the Higgs decay width.

Similarly in Eq. (25), $\langle \sigma \mathrm{v}_{\phi^0\phi^0 \to \chi\bar{\chi}} \rangle$ represents the total annihilation cross section of two ϕ^0 particles into SM particles. The Feynman diagrams of individual processes are shown in Fig. 3 and the expressions of annihilation cross sections for these channels are given below.

$$\langle \sigma \mathrm{v}_{\phi^0\phi^0 \to f\bar{f}} \rangle = \left(\frac{g_{\phi^0\phi^0 h}}{v}\right)^2 \frac{m_f^2}{\pi} \frac{\left(1 - \frac{m_f^2}{m_{\phi^0}^2}\right)^{3/2}}{\left[(4m_{\phi^0}^2 - m_h^2)^2 + (\Gamma_h m_h)^2\right]}\,, \tag{35}$$

$$\langle \sigma \mathrm{v}_{\phi^0\phi^0 \to W^+W^-} \rangle = \frac{1}{2\pi}\left(1 - \frac{m_W^2}{m_{\phi^0}^2}\right)^{1/2} \left[m_{\phi^0}^2 \left(1 - \frac{m_W^2}{m_{\phi^0}^2} + \frac{3m_W^4}{4m_{\phi^0}^4}\right) \left\{ \left(\frac{g_{\phi^0\phi^0 W^+W^-}}{m_W^2}\right)^2 + \right.\right.$$

Interactions involving $XYZ(P)$	$g_{xyz(p)}$
SSh	$g_{SSh} = -\lambda_6 v$
$SShh$	$g_{SShh} = -\frac{1}{2}\lambda_6$
$\phi^0\phi^0 h$	$g_{\phi^0\phi^0 h} = -\alpha v$
$\phi^0\phi^0 hh$	$g_{\phi^0\phi^0 hh} = -\frac{1}{2}\alpha$
$\phi^0\phi^0 W^+W^-$	$g_{\phi^0\phi^0 W^+W^-} = \frac{m_W^2}{v^2}$
$\phi^0\phi^0 ZZ$	$g_{\phi^0\phi^0 ZZ} = \frac{m_Z^2}{2v^2}$
$\phi^0\phi^0\phi^+\phi^-$	$g_{\phi^0\phi^0\phi^+\phi^-} = -\rho_2$
$SS\phi^0\phi^0$	$-\frac{1}{2}\lambda_5$

Table 1: Interactions and the corresponding couplings.

$$
\begin{aligned}
&\frac{\left(\frac{2\, g_{\phi^0\phi^0 h}}{v}\right)^2}{\Big[(4m_{\phi^0}^2 - m_h^2)^2 + (\Gamma_h m_h)^2\Big]} - \frac{\left(\frac{4\, g_{\phi^0\phi^0 h}\;\, g_{\phi^0\phi^0 W^+W^-}}{m_W^2 v}\right)(4m_{\phi^0}^2 - m_h^2)}{\Big[(4m_{\phi^0}^2 - m_h^2)^2 + (\Gamma_h m_h)^2\Big]}\Bigg\} \\
&+\frac{g^2}{4}\Bigg\{ g^2 \left(\frac{m_{\phi^0}(m_W^2 - m_{\phi^0}^2)}{m_W^2(m_{\phi^+}^2 - m_W^2 + m_{\phi^0}^2)}\right)^2 + 2\left(\frac{(m_W^4 - 3m_W^2 m_{\phi^0}^2 + 2m_{\phi^0}^4)}{m_W^4(m_W^2 - m_{\phi^+}^2 - m_{\phi^0}^2)}\right) \\
&\left(g_{\phi^0\phi^0 W^+W^-} - \frac{2\, g_{\phi^0\phi^0 h}(4m_{\phi^0}^2 - m_h^2)\, m_W^2}{v\Big[(4m_{\phi^0}^2 - m_h^2)^2 + (\Gamma_h m_h)^2\Big]}\right)\Bigg\}\Bigg] \quad ,
\end{aligned}
\tag{36}
$$

$$
\begin{aligned}
\langle \sigma \mathrm{v}_{\phi^0\phi^0\to ZZ}\rangle \;=\;& \frac{1}{4\pi}\left(1 - \frac{m_Z^2}{m_{\phi^0}^2}\right)^{1/2}\Bigg[m_{\phi^0}^2\left(1 - \frac{m_Z^2}{m_{\phi^0}^2} + \frac{3m_Z^4}{4m_{\phi^0}^4}\right)\Bigg\{\left(\frac{2\, g_{\phi^0\phi^0 ZZ}}{m_Z^2}\right)^2 + \\
&\frac{\left(\frac{2\, g_{\phi^0\phi^0 h}}{v}\right)^2}{\Big[(4m_{\phi^0}^2 - m_h^2)^2 + (\Gamma_h m_h)^2\Big]} - \frac{\left(\frac{8\, g_{\phi^0\phi^0 h}\;\, g_{\phi^0\phi^0 ZZ}}{m_Z^2 v}\right)(4m_{\phi^0}^2 - m_h^2)}{\Big[(4m_{\phi^0}^2 - m_h^2)^2 + (\Gamma_h m_h)^2\Big]}\Bigg\} \\
&+\frac{g^2}{4\,Cos^2\theta_W}\Bigg\{\frac{g^2}{Cos^2\theta_W}\left(\frac{m_{\phi^0}(m_Z^2 - m_{\phi^0}^2)}{m_Z^2(m_{A^0}^2 - m_Z^2 + m_{\phi^0}^2)}\right)^2 + 2\left(\frac{(m_Z^4 - 3m_Z^2 m_{\phi^0}^2 + 2m_{\phi^0}^4)}{m_Z^4(m_Z^2 - m_{A^0}^2 - m_{\phi^0}^2)}\right) \\
&\left(2\, g_{\phi^0\phi^0 ZZ} - \frac{2\, g_{\phi^0\phi^0 h}(4m_{\phi^0}^2 - m_h^2)\, m_Z^2}{v\Big[(4m_{\phi^0}^2 - m_h^2)^2 + (\Gamma_h m_h)^2\Big]}\right)\Bigg\}\Bigg] \quad ,
\end{aligned}
\tag{37}
$$

$$
\langle \sigma \mathrm{v}_{\phi^0\phi^0\to hh}\rangle \;=\; \frac{1}{4\pi m_{\phi^0}^2}\left(1 - \frac{m_h^2}{m_{\phi^0}^2}\right)^{1/2}\Bigg[\left(\frac{3\, g_{\phi^0\phi^0 h}\; m_h^2}{2v(4m_{\phi^0}^2 - m_h^2)}\right)^2 + g_{\phi^0\phi^0 hh}^2 + \frac{3\, g_{\phi^0\phi^0 h}\;\, g_{\phi^0\phi^0 hh}\;\, m_h^2}{v(4m_{\phi^0}^2 - m_h^2)}
$$

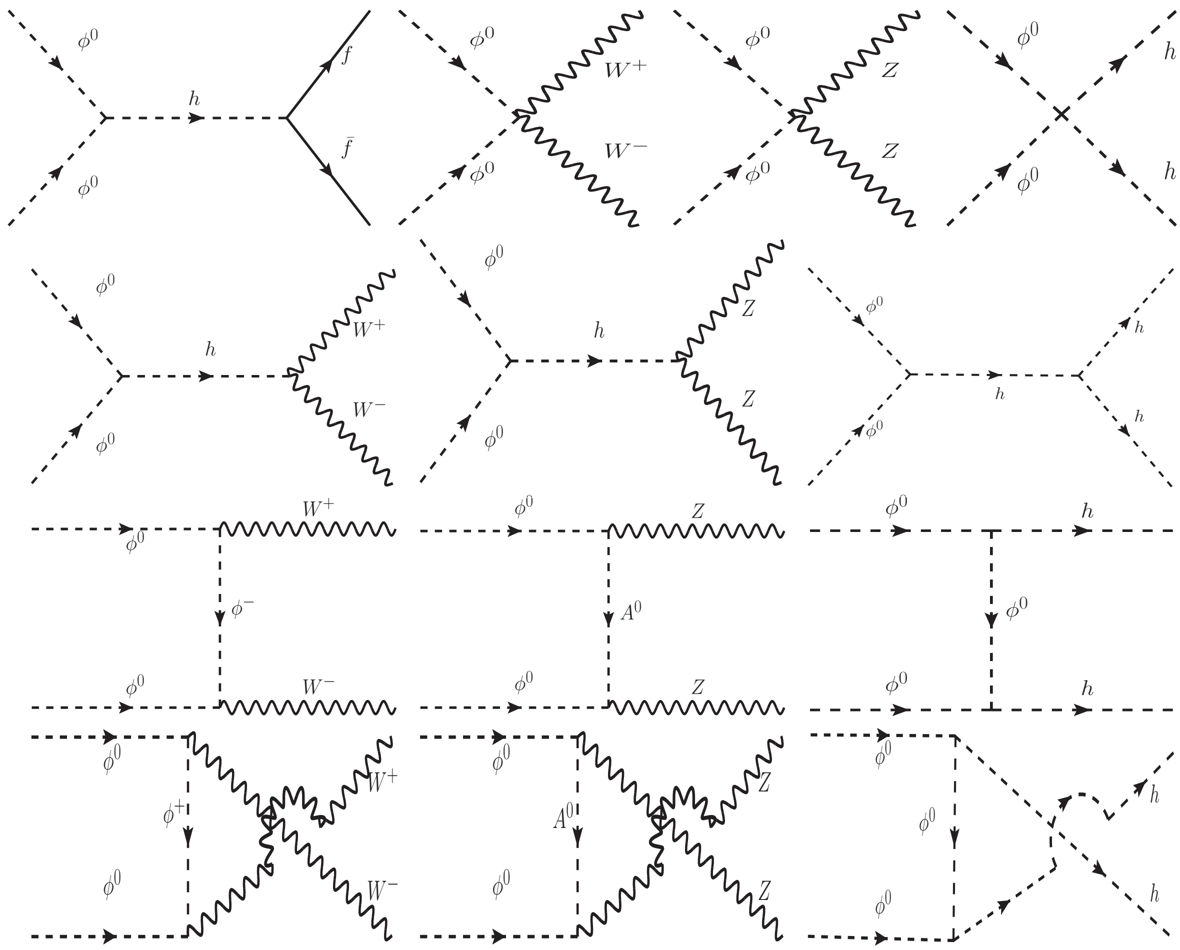

Figure 3: Lowest order Feynman diagrams of two ϕ^0 annihilate into a pair of fermion and anti-fermion, W^+W^-, ZZ and Higgs.

$$+\left(\frac{2\ g^2_{\phi^0\phi^0 h}}{2m^2_{\phi^0}-m^2_h}\right)^2+\frac{4\ g^2_{\phi^0\phi^0 h}g_{\phi^0\phi^0 hh}}{2m^2_{\phi^0}-m^2_h}+\frac{6\ g^3_{\phi^0\phi^0 h}\,m^2_h}{v(2m^2_{\phi^0}-m^2_h)(4m^2_{\phi^0}-m^2_h)}\Bigg]. \tag{38}$$

The other cross section involved in the coupled Boltzmann equations is $\langle\sigma \mathrm{v}_{SS\to\phi^0\phi^0}\rangle$ (due to the presence of the interaction between the two dark matter components S and ϕ^0). The expression for this cross section is given by

$$\begin{aligned}\langle\sigma \mathrm{v}_{SS\to\phi^0\phi^0}\rangle &= \frac{1}{4\pi m^2_S}\left(1-\frac{m^2_{\phi^0}}{m^2_S}\right)^{1/2}\left[\frac{(g_{\phi^0\phi^0 h}\ g_{hSS})^2}{[(4m^2_S-m^2_h)^2+(\Gamma_h m_h)^2]}+g^2_{\phi^0\phi^0 SS}\right.\\ &\left.-\frac{(2\ g_{\phi^0\phi^0 h}\ g_{hSS}\ g_{\phi^0\phi^0 SS})\,(4m^2_S-m^2_h)}{[(4m^2_S-m^2_h)^2+(\Gamma_h m_h)^2]}\right]. \end{aligned} \tag{39}$$

The heavier component of DM is chosen to be S in our case[7]. Since only ϕ^0 will contribute to the 130 GeV gamma ray production (the annihilation cross section $\langle \sigma \mathrm{v}_{SS\to\gamma\gamma} \rangle$ for the singlet S is not enough to produce Fermi-LAT observed 130 GeV $\gamma-$ray flux as we argued before), it's mass should be $m_{\phi^0} \sim 130$ GeV. We will show later that ϕ^0 with its mass ~ 130 GeV can not accommodate the total relic density consistent with the WMAP data. So the rest of the relic density should be provided by the other component S. And we find that it would be a good choice to make $m_S > m_{\phi^0}$. The involvement of this interaction between two dark matter components is a salient feature of our analysis. It would enhance the number density of ϕ^0 through the annihilation of SS during evolution. The Feynman diagrams for this process ($SS \to \phi^0\phi^0$) are given in Fig. 4.

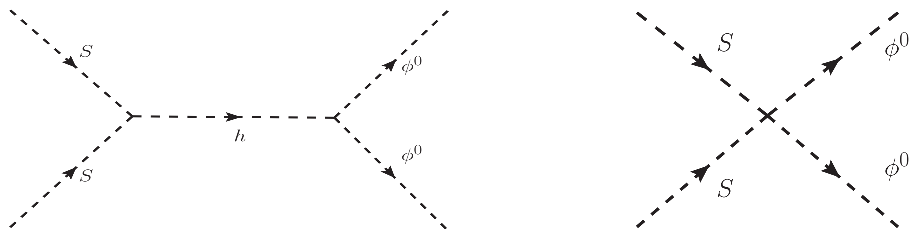

Figure 4: Feynman diagrams for the annihilation channel $SS \to \phi^0\phi^0$

In the left panel of Fig. 5, we have shown the variation of $\langle \sigma \mathrm{v}_{\phi^0\phi^0\to\chi\bar{\chi}} \rangle$ with parameter α (Eq. (11)) for different values of m_{A^0}, namely m_{A^0} = 600 GeV, 500 GeV, 400 GeV, 350 GeV, 300 GeV. In the right panel, the variation of $\langle \sigma \mathrm{v}_{SS\to\chi\bar{\chi}} \rangle$ with parameter λ_6 (Eq. (3)) is shown. We have chosen $m_{\phi^0} = m_{\phi^+} = 130$ GeV, α = -0.037 and $m_S = 130.5$ GeV for drawing these plots. The reason behind this choice of parameters should be cleared in the next section.

4 Calculation of Model Parameters

In this section we describe the procedure adopted in this work in order to estimate the values of the parameters involved in our proposed model. At the very outset, we summarise few basic requirements. In the present two component dark matter model, only the component ϕ^0 can account for the observed 130 GeV γ-line through the annihilation channel $\phi^0\phi^0 \to \gamma\gamma$ details of which is discussed in the next section. This is due to the fact that the other component S being a scalar singlet cannot produce sufficient annihilation cross section for the channel $SS \to \gamma\gamma$.

[7] If $m_S < m_{\phi^0}$, ϕ^0 component would be annihilated into S (via the process $\phi^0\phi^0 \to SS$). This would reduce the contribution of ϕ^0 to the combined relic density and hence the $\gamma-$ray flux originated from $\phi^0\phi^0$ annihilation would be suppressed.

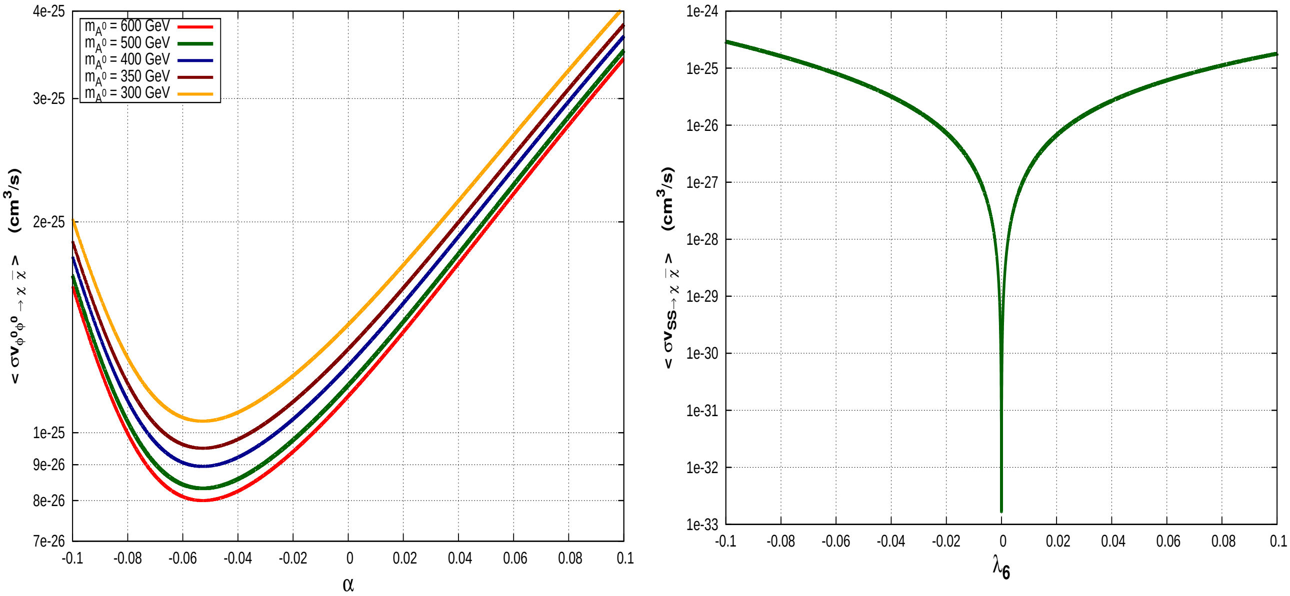

Figure 5: Left panel - Variation of $\langle \sigma \mathrm{v}_{\phi^0\phi^0 \to \chi\bar{\chi}} \rangle$ with α for different values of m_{A^0}, Right panel - Variation of $\langle \sigma \mathrm{v}_{SS \to \chi\bar{\chi}} \rangle$ with λ_6 for $m_S = 130.5$ GeV.

So we conclude that the mass of the ϕ^0 component needs to be ~ 130 GeV. We also find that a choice for the mass of the charged scalars, $\phi^{\pm}$ (involved in the loop of the $\phi^0\phi^0 \to \gamma\gamma$ process) close to m_ϕ enhances the annihilation cross section $\langle \sigma \mathrm{v}_{\phi^0\phi^0 \to \gamma\gamma} \rangle$ (see Eq.(46)).Therefore, in order to maximise this contribution (required to achieve the cross section in the right ball park without taking a very high value for the relevant parameter in the model), we consider $m_{\phi^0} \simeq m_{\phi^\pm} = 130$ GeV throughout the present discussion. Note that such a choice is consistent with the LEP bound [30]. With this consideration, the parameter α is reduced to $\lambda_1/2$.

Of course ϕ^0 with $m_{\phi^0} = 130$ GeV cannot individually account for the WMAP results on relic density. In our scenario, this deficit will be compensated by the contribution of the other component S. However we need to maximise the contribution of ϕ^0 to the combined relic density so as to keep the flux of the observed gamma ray (130 GeV) from the Galactic centre at an adequate level (see Eqs.(42, 52)). For example if ϕ^0 contributes to 60% compared to a case where it contributes only 30% to the total relic density then the flux for the gamma ray originated from DM annihilation will also be proportionately higher compared to the latter case. Apart from the WMAP data, we also use the limits obtained from the dark matter direct detection experiments. Needless to mention that in doing so the conditions obtained in Eqs. (12-16, 17, 18) are always satisfied.

In order to find a choice of parameter space for which the contribution from ϕ^0 toward relic density can be maximised, we calculate the ratio $\left(\frac{\Omega_{\phi^0} h^2}{\Omega_c h^2}\right)$. The relic densities $\Omega_{\phi^0} h^2$ and $\Omega_c h^2$

are computed using Eqs. (26, 27, 29). In the left panel of Fig. 6 we plot $\left(\frac{\Omega_{\phi^0}h^2}{\Omega_c h^2}\right)_{\text{Maximum}}$, as a function of the parameter α for different values of m_{A^0}. Here by $\left(\frac{\Omega_{\phi^0}h^2}{\Omega_c h^2}\right)_{\text{Maximum}}$, we mean that we have chosen only the largest possible value of the ratio corresponding to a particular α while other parameters are scanned over their entire range ($-0.1 \leq \lambda_6 \leq 0.1$, $0.1 \leq \lambda_5 \leq 1.0$). The limits of α (Eqs. (22, 23)) obtained from XENON 100 (2012) data and XENON 100 (2011) data are superimposed on this figure (left panel of Fig. 6)) to find out the allowed region for the ratio, $\left(\frac{\Omega_{\phi^0}h^2}{\Omega_c h^2}\right)$.

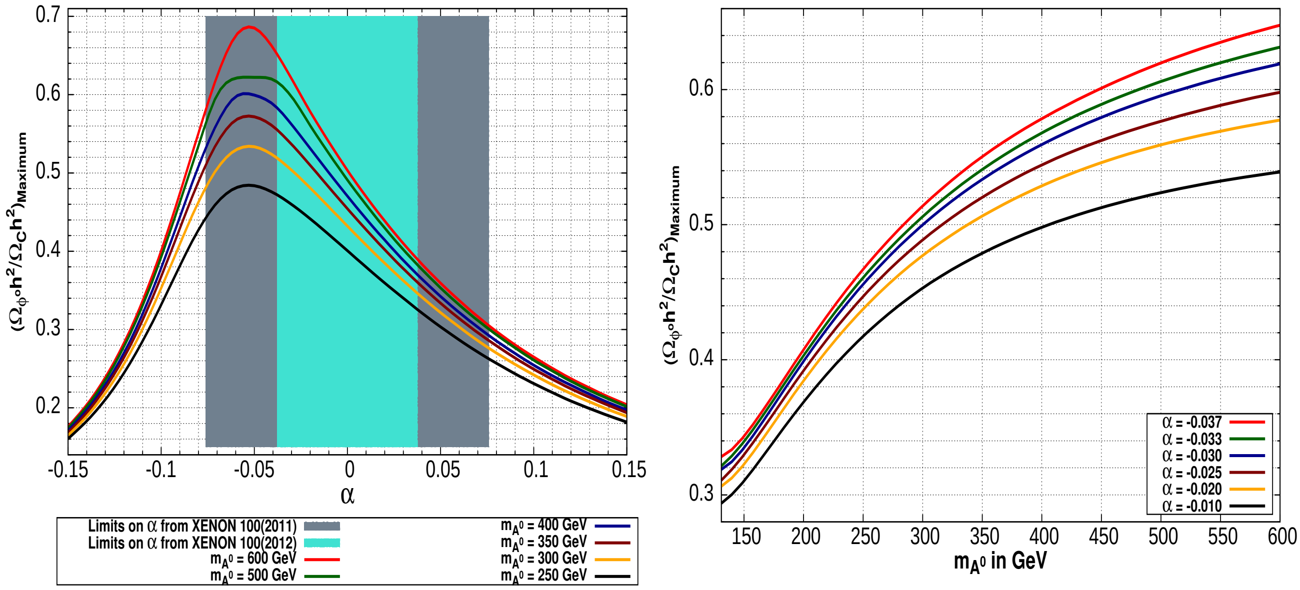

Figure 6: Left panel - Variations of $\left(\frac{\Omega_{\phi^0}h^2}{\Omega_c h^2}\right)_{\text{Maximum}}$ with parameter α for different values of m_{A^0}, Right panel - Variations of $\left(\frac{\Omega_{\phi^0}h^2}{\Omega_c h^2}\right)_{\text{Maximum}}$ with m_{A^0} for different values of parameter α.

In the left panel of Fig. 6 the slategray colour band represent the limits on α ($|\alpha| \leq 0.076$) obtained from XENON 100 (2011) data while the limits on α (Eq. 22) from XENON 100 (2012) data are depicted in the figure with the turquoise colour band. We want to find a suitable value of α (arguably from the region allowed by XENON 100 (2012), as then the other bounds will also be satisfied automatically) for which we get a maximum contribution to the ratio $\left(\frac{\Omega_{\phi^0}h^2}{\Omega_c h^2}\right)$. Note that this ratio depends on the choice of m_{A^0}. In order to have more insight on this dependence, we show the variations of $\left(\frac{\Omega_{\phi^0}h^2}{\Omega_c h^2}\right)_{\text{Maximum}}$ with m_{A^0} for different values of α (which are allowed by XENON 100 (2012) data) in the right panel of Fig. 6. It is evident the contribution of ϕ^0 increases as m_{A^0} increases. This can also be noted from the same figure that for a fixed value of α, the increase of $\Omega_{\phi^0}h^2$ with m_{A^0} is stripper for lower values of m_{A^0}. However we cannot

choose a value of m_{A^0} which is arbitrarily large since our choice $m_{\phi^0} = m_{\phi^\pm} = 130$ GeV imposes a relation between parameters λ_2 and λ_3. For example, to achieve $m_{A^0} = 500$ GeV, we find $\lambda_2 = 3.852$, $\lambda_3 = -1.926$ when $\alpha =$ -0.037 is considered (fixing λ_2 and λ_3 will be discussed later in the context of Fig. 7). Taking into consideration all the above discussions we can have the contribution of ϕ^0 to the total relic density to be at most $\lesssim 62\%$. A choice of $m_{A^0} = 900$ GeV would require a value of $\lambda_2 \sim 4\pi$, which poses a threat to the perturbativity. Therefore in the present work we consider $m_{A^0} \lesssim 500$ GeV and the corresponding parameters as obtained following the discussions above.

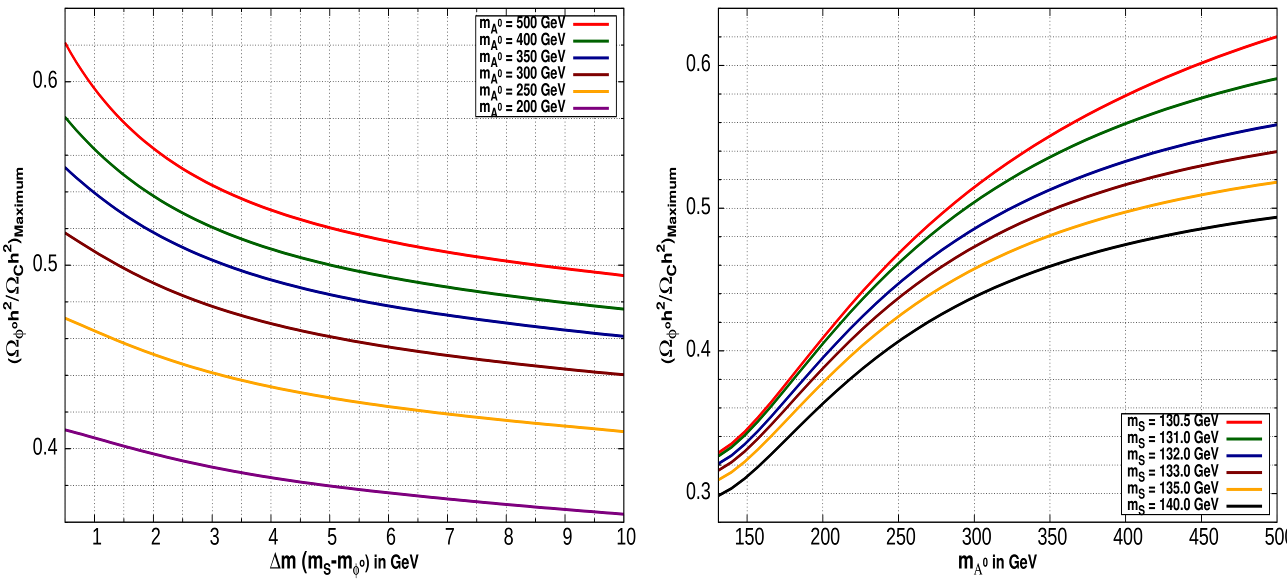

Figure 7: Left panel - Variations of $\left(\frac{\Omega_{\phi^0}h^2}{\Omega_c h^2}\right)_{\text{Maximum}}$ with $\Delta m(m_S - m_{\phi^0})$ for different values of m_{A^0}, Right panel - Variations of $\left(\frac{\Omega_{\phi^0}h^2}{\Omega_c h^2}\right)_{\text{Maximum}}$ with m_{A^0} for different values of $\Delta m(m_S - m_{\phi^0})$.

As it is now evident that the inert doublet component alone with $m_{\phi^0} = 130$ GeV cannot account for the total dark matter content of the universe and one needs to add the relic density of the singlet component S for producing the WMAP satisfied total relic density. In fact this is one of the motivations for choosing this two component (inert doublet + scalar singlet dark matter model). In order to choose a suitable mass for S in the present two component dark matter model, we define a quantity Δm $(= m_S - m_{\phi^0})$ remembering that m_S should be heavier than m_{ϕ^0} as discussed before. We then study the variations of $\left(\frac{\Omega_{\phi^0}h^2}{\Omega_c h^2}\right)_{\text{Maximum}}$ with Δm for different values of m_{A^0} which is shown in the left panel of Fig. 7. In the right panel of Fig. 7 we show the variations of the fraction $\left(\frac{\Omega_{\phi^0}h^2}{\Omega_c h^2}\right)_{\text{Maximum}}$ with m_A^0 (≤ 500 GeV) for different values of m_S. The plots in both the panels are obtained with $\alpha = -0.037$ (which satisfy both XENON

data). Comparing both the panels of Fig. 7 one concludes that the contribution of ϕ^0 to the combined relic density increases as the mass splitting between the two components of the dark matter decreases and the ratio $\left(\frac{\Omega_{\phi^0}h^2}{\Omega_c h^2}\right)_{\rm Maximum}$ is $\sim$ 62% for Δm = 0.5 GeV and m_{A^0} = 500 GeV.

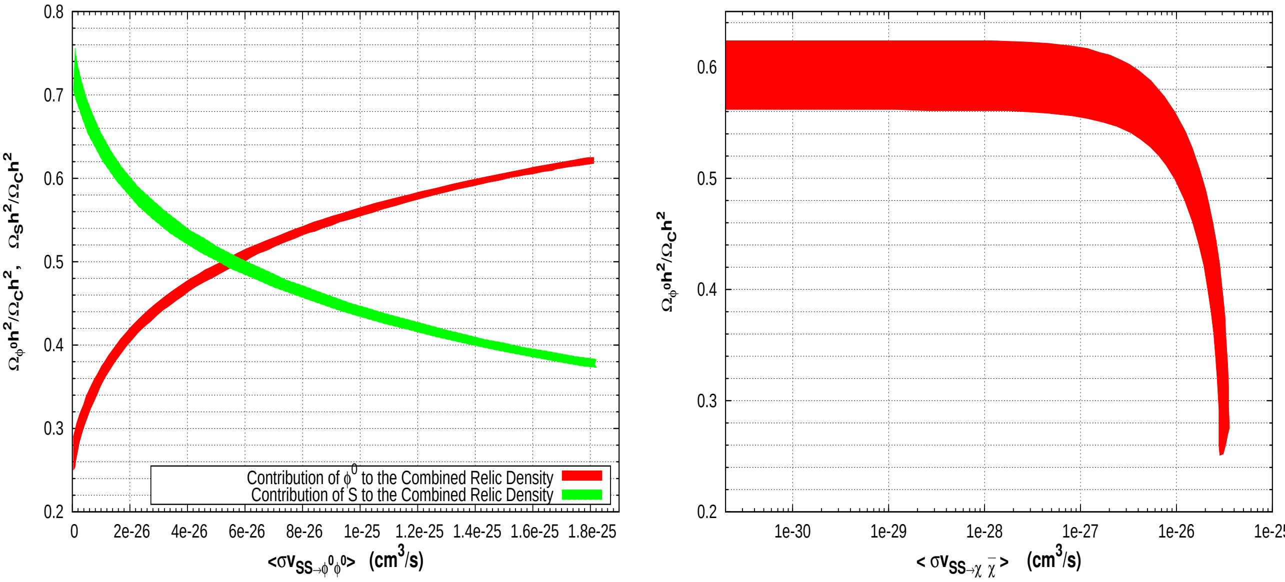

Figure 8: Left panel - Variations of the contributions of S ($\Omega_S h^2$) and ϕ^0 ($\Omega_{\phi^0}h^2$) to the combined relic density ($\Omega_c h^2$) with the annihilation cross section $\langle\sigma {\rm v}_{SS\to\phi^0\phi^0}\rangle$, Right panel - Variations of the contributions of ϕ^0 ($\Omega_{\phi^0}h^2$) to the combined relic density ($\Omega_c h^2$) with the annihilation cross section $\langle\sigma {\rm v}_{SS\to\chi\bar{\chi}}\rangle$.

We also calculate the variations of $\left(\frac{\Omega_{\phi^0}h^2}{\Omega_c h^2}\right)$ and $\left(\frac{\Omega_S h^2}{\Omega_c h^2}\right)$ with the cross section $\langle\sigma {\rm v}_{SS\to\phi^0\phi^0}\rangle$ and the results are plotted in the left panel of Fig. 8. In all these of calculations, we have used our standard set of parameters, $m_{\phi^0} = m_{\phi^+}$ = 130 GeV, m_S = 130.5 GeV, α = -0.037, m_{A^0} = 500 GeV (as mentioned earlier). From this plot, it is clear that initially when $\langle\sigma {\rm v}_{SS\to\phi^0\phi^0}\rangle$ is very small (or nearly zero) the contribution of ϕ^0 is only $\sim$ 25% of the combined relic density. This is because for small values of $\langle\sigma {\rm v}_{SS\to\phi^0\phi^0}\rangle$, Eqs. (26, 27) effectively become two decoupled equations that represent the Boltzmaan's equations for RSDM and IDM respectively. Under such circumstance, the calculations of the individual contributions for S and ϕ^0 are pursued .

Note that in this decoupled scenario, individual relic density contribution would be inversely proportional to the corresponding annihilation cross section. Therefore we need to have an estimate for $\langle\sigma {\rm v}_{\phi^0\phi^0\to\chi\bar{\chi}}\rangle$ and $\langle\sigma {\rm v}_{SS\to\chi\bar{\chi}}\rangle$. In order to understand this in more detail, we refer to Fig. 5. From the left panel of Fig. 5, we see that the value of $\langle\sigma {\rm v}_{\phi^0\phi^0\to\chi\bar{\chi}}\rangle$ is $\sim 8.5\times10^{-26}$ cm^3/s for m_{A^0} = 500 GeV, $\alpha = -0.037$, $m_{\phi^0} = m_{\phi^+}$ = 130 GeV. This value of $\langle\sigma {\rm v}_{\phi^0\phi^0\to\chi\bar{\chi}}\rangle$ is nearly

4 times larger than what is required to get WMAP satisfied relic density for dark matter mass of 130 GeV, thereby contributing only $\sim 25\%$ to the total relic density (Eq. (19)) as seen from left panel of Fig. 8. So we would expect that the rest $\sim 75\%$ contribution should come from the singlet scalar component S in the present model. This is indeed possible if we consider the right panel of Fig. 5. This corresponds to a case where practically there is no interactions between S and ϕ^0, i.e. $\lambda_5 \simeq 0$. As the interaction between S and ϕ^0 becomes increasingly stronger (i.e. $|\lambda_5|$ starts to have nonzero value), more and more S particles annihilate to produce ϕ^0 particles and contribution of ϕ^0 to the combined relic density will be boosted. It reaches a maximum which comes out to be 62% in our present analysis for $\langle \sigma \mathrm{v}_{SS\to\phi^0\phi^0}\rangle \sim 1.8 \times 10^{-25}\mathrm{cm}^3/\mathrm{s}$ as seen from the left panel of Fig. 8.

The right panel of Fig. 8 shows the variation of $\left(\frac{\Omega_{\phi^0}h^2}{\Omega_c h^2}\right)$ with $\langle \sigma \mathrm{v}_{SS\to\chi\bar{\chi}}\rangle$. It indicates that contribution of ϕ^0 decreases as the value of $\langle \sigma \mathrm{v}_{SS\to\chi\bar{\chi}}\rangle$ increases. This is because of the increment of $\langle \sigma \mathrm{v}_{SS\to\chi\bar{\chi}}\rangle$ signifies large number S particles annihilate into SM particles and consequently less number of particles are available for annihilation of S to produce ϕ^0 in the final state. As a result the relic density of ϕ^0 decreases. From this plot, we conclude that in order to obtain the relic density contribution of ϕ^0 close to 62% or above the value of $\langle \sigma \mathrm{v}_{SS\to\chi\bar{\chi}}\rangle$ should be $\lesssim 1.74 \times 10^{-28}\mathrm{cm}^3/\mathrm{s}$. Note that $\langle \sigma \mathrm{v}_{SS\to\chi\bar{\chi}}\rangle$ involves the parameter λ_6 and λ_5, λ_6 both of which are involved in $\langle \sigma \mathrm{v}_{SS\to\phi^0\phi^0}\rangle$. Therefore this limit (on $\langle \sigma \mathrm{v}_{SS\to\chi\bar{\chi}}\rangle$) along with the other one we just discussed above, $\langle \sigma \mathrm{v}_{SS\to\phi^0\phi^0}\rangle \sim 1.8 \times 10^{-25}\mathrm{cm}^3/\mathrm{s}$, set up a range of allowed region of λ_5 and λ_6 if we restrict ourselves with $\left(\frac{\Omega_{\phi^0}h^2}{\Omega_c h^2}\right) \sim 62\%$. The allowed range of values of parameters λ_5, λ_6 for the present case ($m_{A^0} = 500$ GeV) is shown in Fig. 9. In Table 2 we furnish the values of the parameters λ_5 and λ_6 along with other model parameters.

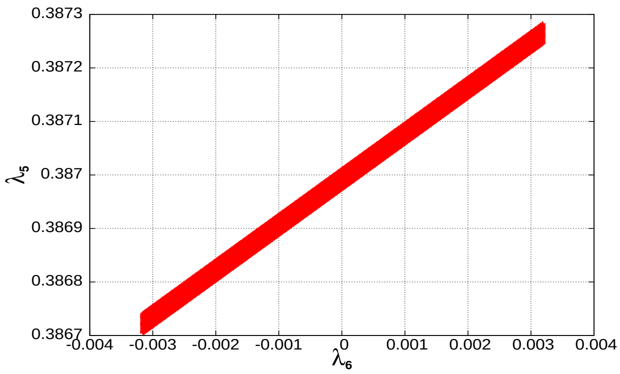

Figure 9: Allowed range of the parameters λ_5, λ_6 in order to obtain $\langle \sigma \mathrm{v}_{SS\to\chi\bar{\chi}}\rangle \leq 1.74 \times 10^{-28}\mathrm{cm}^3/\mathrm{s}$ and $\langle \sigma \mathrm{v}_{SS\to\phi^0\phi^0}\rangle \sim 1.8 \times 10^{-25}\mathrm{cm}^3/\mathrm{s}$ such that the contribution of ϕ^0 component is maximum to the combined relic density for $m_{\phi^0} = m_{\phi^+} = 130$ GeV, $\Delta m = 0.5$ GeV, $\alpha = -0.037$, $m_{A^0} = 500$ GeV.

Mass of A^0 (m_A^0) (GeV)	Contribution of ϕ^0 in the combined Relic Density	μ_2 (GeV)	λ_1	λ_5	$\|\lambda_6\|$	λ_2	λ_3
300	51.7%	138.344	-0.074	0.2698 - 0.2703	$\leq 2.6 \times 10^{-3}$	1.208	-0.604
350	55.3%	138.344	-0.074	0.3014 - 0.3020	$\leq 2.8 \times 10^{-3}$	1.745	-0.872
400	58.1%	138.344	-0.074	0.3322 - 0.3327	$\leq 2.8 \times 10^{-3}$	2.365	-1.182
500	62.1%	138.344	-0.074	0.3867 - 0.3873	$\leq 3.2 \times 10^{-3}$	3.852	-1.926

Table 2: Relic density contribution of ϕ^0 for different values of m_A^0 and the corresponding values of model parameters for $\alpha = -0.037$, $\Delta m = 0.5$ GeV ($m_S = 130.5$ GeV, $m_{\phi^0} = 130.0$ GeV).

5 130 GeV γ-ray line from Dark Matter annihilation

In this section our endeavour will be to explain the recently observed 130 GeV γ-line from the Galactic centre originated from dark matter annihilation in the framework of the present two component dark matter model. In order to produce such a 130 GeV γ-line, the required DM annihilation cross section into two photons should be $\sim 10^{-27}$ cm^3/s as predicted from the analysis [1, 2] of Fermi-LAT data [3]. In the context of the present two component dark matter model, only the ϕ^0 component having mass 130 GeV can contribute to the production of 130 GeV $\gamma-$ray line. The annihilation of $\phi^0\phi^0$ into $\gamma\gamma$ can take place only via charged scalar $\phi^\pm$ and $W^\pm$ loops. It can indeed produce the required cross section $\sim 10^{-27}$ cm^3/s. The cross sections for other annihilation channels that can produce $\gamma\gamma$ (e.g. via Higgs) for both the components ϕ^0 and S are orders of magnitude less than this value [10].

We calculate the γ-ray flux due to annihilation of ϕ^0 in the "central region" of our Milky way galaxy. The lowest order Feynman diagrams for the process $\phi^0\phi^0 \to \gamma\gamma$ via $\phi^\pm$ and $W^\pm$ loops are shown in Fig. 10. The expression of differential $\gamma-$ray flux due to dark matter annihilation in galactic halo is given by [31],

$$\frac{d\Phi_\gamma}{dE_\gamma} = \frac{1}{8\pi}\frac{\langle \sigma {\rm v}_{\phi^0\phi^0\to\gamma\gamma}\rangle}{m^2_{\phi^0}}\frac{dN_\gamma}{dE_\gamma} r_\odot \rho_\odot^2 \bar{J} \ , \tag{40}$$

where $r_\odot = 8.5$ kpc is the distance of the sun from the Galactic centre and $\rho_\odot = 0.4$ GeV/cm^3 is the the local dark matter density at the solar neighbourhood. The quantity $\bar{J}$ in the above is given by

$$\bar{J} = \frac{4}{\Delta\Omega}\int dl \int db \ \cos b \ J(l,b) \ , \tag{41}$$

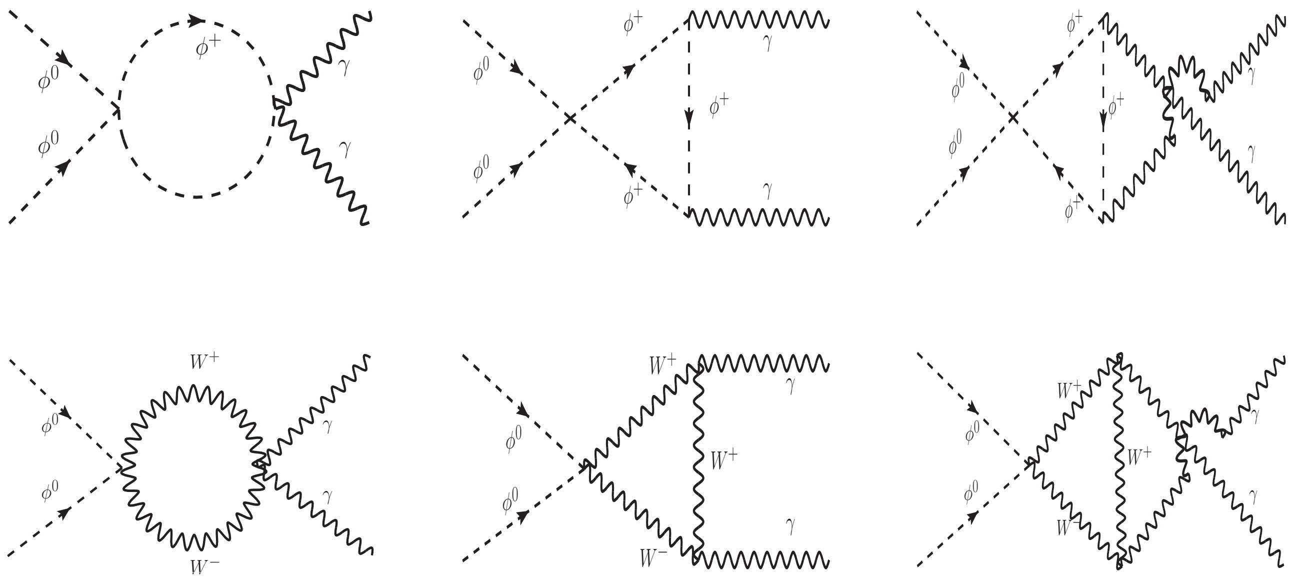

Figure 10: Lowest order Feynman diagrams for the process $\phi^0\phi^0 \to \gamma\gamma$

with

$$J(l,b) = \int_{l.o.s} \frac{ds}{r_\odot} \left(\frac{\rho(r)}{\rho_\odot} \right)^2 \ , \tag{42}$$

and

$$\Delta\Omega = 4 \int dl \int db \ \cos b \ . \tag{43}$$

Here l and b in Eqs. (41, 43) are galactic longitude and latitude respectively. In the above, the integration is performed around a radius of 3^o (galactic central region) around a centre with coordinates $(l,\, b) = (-1^o\ ,\, -0.7^o)$ [2]. In Eq. (42) r and s are related by,

$$r = \left(s^2 + r_\odot^2 - 2 s r_\odot \cos l \cos b \right)^{1/2} \ . \tag{44}$$

The expression of the energy spectrum of γ, denoted by $\frac{dN_\gamma}{dE_\gamma}$ is given by,

$$\frac{dN_\gamma}{dE_\gamma} = 2\delta(E - E_\gamma) \ . \tag{45}$$

We have performed l, b integration (in Eqs. (41, 43)) over the "central region" of our galaxy and the s integration (in Eq. 42) is along the line of sight (l.o.s).

We explicitly calculate all the Feynman diagrams given in Fig. 10 and obtain the expression for $\langle \sigma \mathrm{v}_{\phi^0\phi^0\to\gamma\gamma} \rangle$ as

$$\langle \sigma \mathrm{v}_{\phi^0\phi^0\to\gamma\gamma} \rangle = \frac{\alpha^2 \ m_{\phi^0}^2}{32\pi^3} \left| \frac{g_{\phi^0\phi^0\phi^+\phi^-} F_{\phi^+}}{m_{\phi^+}^2} - \frac{g_{\phi^0\phi^0 W^+ W^-} F_W}{m_W^2} \right|^2 \ . \tag{46}$$

Where

$$\begin{aligned} F_{\phi^+} &= \tau[1-\tau f(\tau)] \\ F_W &= 2+3\tau+2\tau(2-\tau)f(\tau). \end{aligned} \tag{47}$$

with $\tau = \frac{4m_i^2}{m_{\phi^0}^2}$, $\qquad i = \phi^\pm, W^\pm$, and

$$f(\tau) = \begin{cases} \left[\sin^{-1}(\sqrt{1/\tau})\right]^2, & \text{for} \quad \tau \geq 1\,, \\ -\frac{1}{4}\left[\ln\frac{1+\sqrt{1-\tau}}{1-\sqrt{1-\tau}} - i\pi\right]^2, & \text{for} \quad \tau < 1\,. \end{cases} \tag{48}$$

Since the couplings $g_{\phi^0\phi^0\phi^+\phi^-} = -\rho_2$ and $g_{\phi^0\phi^0W^+W^-} = \frac{m_W^2}{v^2}$ (Table 1), Eq. (46) can be written as

$$\langle \sigma \mathrm{v}_{\phi^0\phi^0\to\gamma\gamma}\rangle = \frac{\alpha^2\, m_{\phi^0}^2}{32\pi^3}\left|\frac{\rho_2 F_{\phi^+}}{m_{\phi^+}^2} + \frac{F_W}{v^2}\right|^2 . \tag{49}$$

In the present work, γ-ray flux is calculated for two different dark matter halo profiles namely the NFW profile [17] and the Einasto profile [18]. These halo profiles give the functional dependence of dark matter density $\rho(r)$ with r. The expression of $\rho(r)$ for the NFW profile is given by,

$$\rho_{\mathrm{NFW}}(r) = \frac{\rho_s}{(r/r_s)\,(1+r/r_s)^2} \tag{50}$$

and for the Einasto profile

$$\rho_{\mathrm{Einasto}}(r) = \rho_s \exp\left\{-\frac{2}{\gamma}\left[\left(\frac{r}{r_s}\right)^\gamma - 1\right]\right\}\ , \tag{51}$$

where r_s in Eqs. (50-51) is taken to be 20 kpc and $\gamma = 0.17$ in Eq. (51). In the above the value of the normalisation constant ρ_s is determined by demanding that at $r = r_\odot$, the density $\rho(r) = \rho_\odot$. We have seen earlier that in the present model of two component dark matter, the inert doublet component ϕ^0 contributes to $\sim 62\%$ $\left(\frac{\Omega_{\phi^0}h^2}{\Omega_c h^2} \sim 0.62\right)$ of the total dark matter relic density. Therefore in calculating the $\gamma-$ray flux from the process $\phi^0\phi^0 \to \gamma\gamma$ we compute ρ_s by taking

$$\rho'_\odot = \rho_\odot \times \frac{\Omega_{\phi^0}h^2}{\Omega_c h^2}, \tag{52}$$

and demanding that for the dark matter component ϕ^0, $\rho(r) = \rho'_\odot$ at $r = r_\odot$ with $\rho_\odot = 0.4$ GeV/cm^3 [32].

Mass of A^0 (GeV)	$\left(\frac{\Omega_{\phi^0}h^2}{\Omega_c h^2}\right)$	$\rho'_\odot$ (GeV/cm^3)	ρ_s (GeV/cm^3)	$\langle\sigma \mathrm{v}_{\phi^0\phi^0\to\gamma\gamma}\rangle$ (cm^3/s)	ρ_2
500	0.621	0.248	0.214	$1.183^{+0.407}_{-0.342}\times 10^{-27}$	$4.74^{+0.64}_{-0.64}$
400	0.581	0.232	0.201	$1.341^{+0.456}_{-0.389}\times 10^{-27}$	$5.00^{+0.67}_{-0.68}$
350	0.553	0.221	0.191	$1.489^{+0.504}_{-0.436}\times 10^{-27}$	$5.23^{+0.70}_{-0.74}$
300	0.517	0.207	0.178	$1.710^{+0.580}_{-0.497}\times 10^{-27}$	$5.55^{+0.75}_{-0.76}$

Table 3: Results for the NFW Profile.

From the left panel of Fig. 3 of Ref. [2] the best fit value of the $\gamma-$ray flux (in terms of $E^2\Phi$ (GeV cm^{-2} s^{-1} sr^{-1})) observed by Fermi-LAT from the central signal region of the Galaxy can be read as $E^2\Phi = 5.6\times 10^{-5}$ GeV cm^{-2} s^{-1} sr^{-1} with 95% C.L. error band that lies in the range $3.97\times 10^{-5} \le E^2\Phi \le 7.51\times 10^{-5}$ (GeV cm^{-2} s^{-1} sr^{-1}). We use these values of the flux in Eq. (40) and compute $\langle\sigma \mathrm{v}_{\phi^0\phi^0\to\gamma\gamma}\rangle$ for the best fit value of the flux as also the two extremities of its error band at 130 GeV. Note that the parameter ρ_2 is yet to be determined. This can be estimated by calculating the cross section $\langle\sigma \mathrm{v}_{\phi^0\phi^0\to\gamma\gamma}\rangle$ (given by Eq. (49)) and hence the flux $E^2\Phi$ and then comparing this flux with that given by the Fermi-LAT data.

The results are furnished in Table 3 and Table 4 for the NFW profile and the Einasto profile respectively. They are given for the chosen mass m_{A^0} of 500 GeV as also for three other values of m_{A^0} namely 400, 350, 300 GeV for the purpose of demonstration. In both the Tables 3, 4 the values of the cross sections obtained for the best fit value of the flux are given. The computed cross sections for the two extremities of the error band of the flux are shown by the subscripts and superscripts of the central values. The corresponding values of ρ_2 that are calculated using Eq. (49) are also shown in similar fashion. It is seen from both the Tables that although the calculated values for ρ_2 depend on the dark matter density profile that one chooses, they are

Mass of A^0 (GeV)	$\left(\frac{\Omega_{\phi^0}h^2}{\Omega_c h^2}\right)$	$\rho'_\odot$ (GeV/cm^3)	ρ_s (GeV/cm^3)	$\langle\sigma \mathrm{v}_{\phi^0\phi^0\to\gamma\gamma}\rangle$ (cm^3/s)	ρ_2
500	0.621	0.248	0.051	$0.608^{+0.205}_{-0.179}\times 10^{-27}$	$3.57^{+0.47}_{-0.50}$
400	0.581	0.232	0.047	$0.712^{+0.244}_{-0.206}\times 10^{-27}$	$3.82^{+0.51}_{-0.52}$
350	0.553	0.221	0.045	$0.780^{+0.267}_{-0.226}\times 10^{-27}$	$3.97^{+0.53}_{-0.54}$
300	0.517	0.207	0.042	$0.896^{+0.305}_{-0.263}\times 10^{-27}$	$4.21^{+0.56}_{-0.58}$

Table 4: Results for the Einasto Profile.

within the perturbative limit and the corresponding cross sections $\langle\sigma \mathrm{v}_{\phi^0\phi^0\to\gamma\gamma}\rangle$ are also within the desired limits of $\sim 10^{-27}$ cm^3/s.

Here we like to mention that we have checked the possibility that the continuum gamma-rays may overshoot the monochromatic gamma-ray line. In Ref. [6], the authors have shown that in order to distinguish the monochromatic gamma-line (from DM DM $\to\gamma\gamma$ channel) from the continuum gamma-ray spectrum (produced by the secondary photons originating from the annihilation products of dark matter e.g. gauge bosons, $q\bar{q}$, $f\bar{f}$), the branching ratio for the channel DM DM $\to\gamma\gamma$ must be greater than 1% of total annihilation cross section (sum of annihilation cross sections for all possible channels). For the dark matter component ϕ^0 in our model we find that this ratio is nearly 1/70 (i.e. $> 10^{-2}$) as seen from the left panel of Fig. 5 and Table 3.

6 Discussions and Conclusions

In the present work we propose a dark matter model which contains two dark matter candidates. Such a two component dark matter model can be obtained by adding a scalar singlet S (singlet

under SM gauge group) and a doublet Φ (doublet under SM gauge group) to the scalar sector of SM. We have introduced discrete symmetry $\mathrm{Z}_2 \times \mathrm{Z}_2'$ under which only S and Φ transform non-trivially. Both the scalar singlet S and doublet Φ do not produce any VEV. Consequently $\mathrm{Z}_2 \times \mathrm{Z}_2'$ symmetry remains unbroken which ensure the stability of both the components (S, ϕ^0) of the dark matter in the present model. While the component ϕ^0 (neutral part of the doublet Φ) can produce the annihilation cross section required to obtain 130 GeV γ-line, the value of the corresponding cross section for the scalar singlet component S falls deficit by few orders of magnitude. However the component ϕ^0 above, having a mass of 130 GeV cannot solely account for the relic density predicted by WMAP. This deficit in relic density is compensated by the scalar singlet component S such that the combined relic density $(\Omega_c h^2)$ for this two component dark matter model always lies within the range given by WMAP. Combined relic density is the sum of individual relic densities of both the components S and ϕ^0 which are obtained by solving the coupled Boltzmann's equations numerically. We have found that the contribution of the component ϕ^0 to $\Omega_c h^2$ will be maximum ($\sim 62\%$) when we consider $\alpha = -0.037$, $|\lambda_6| \leq 3.2 \times 10^{-3}$ (both satisfy XENON 100 (2012) limit as well as limits from other dark matter direct detection experiments namely CDMS-II, EDELWEISS-II etc.), $\Delta m = 0.5$ GeV, $\lambda_5 \sim 0.387$ and $m_{A^0} = 500$ GeV. Finally in the last section we have calculated the annihilation cross section $\langle \sigma \mathrm{v}_{\phi^0\phi^0 \to \gamma\gamma} \rangle$ for the channel $\phi^0\phi^0 \to \gamma\gamma$ with the mass of $\phi^0 \sim 130$ GeV. Using the expression of this annihilation cross section ($\langle \sigma \mathrm{v}_{\phi^0\phi^0 \to \gamma\gamma} \rangle$) we have computed the $\gamma-$ray flux of energy 130 GeV for two different dark matter halo profiles namely the NFW profile and the Einasto profile. The exact dark matter density at the galactic centre is unknown (e.g. Ref. [31] and references therein). This may produce an additional uncertainty in the flux calculation. Depending on the value of the dark matter density at the galactic centre, 130 GeV gamma-line may also be produced for a value of annihilation cross section lower than the specified value of $\sim 10^{-27}$ cm^3/s. Fermi Collaboration placed an upper limit [33] $\sigma \mathrm{v}_{\gamma\gamma} < 1.4 \times 10^{-27}$ cm^3/s for 130 GeV dark matter with an NFW profile and $\sigma \mathrm{v}_{\gamma\gamma} < 1.0 \times 10^{-27}$ cm^3/s with an Einasto profile. In the present work we indeed obtain $\sigma \mathrm{v}_{\gamma\gamma}$ in the range of this upper limit ($\sim 10^{-27}$ cm^3/s).

Acknowledgments : A.B. would like to thank A. Ghosal and D. Adak for useful suggestions and discussions. The authors thank J. Kopp, M. Raidal and K. Kannike for very useful suggestions and comments. A.S acknowledges the support from the Start Up grant from IIT Guwahati.

References

[1] T. Bringmann, X. Huang, A. Ibarra, S. Vogl and C. Weniger, JCAP **1207**, 054 (2012) [arXiv:1203.1312 [hep-ph]], C. Weniger, JCAP **1208**, 007 (2012) [arXiv:1204.2797 [hep-ph]].

[2] E. Tempel, A. Hektor and M. Raidal, JCAP **1209**, 032 (2012) [Addendum-ibid. **1211**, A01 (2012)] [arXiv:1205.1045 [hep-ph]].

[3] W. B. Atwood *et al.* [LAT Collaboration], Astrophys. J. **697**, 1071 (2009) [arXiv:0902.1089 [astro-ph.IM]].

[4] J. M. Cline, Phys. Rev. D **86**, 015016 (2012) [arXiv:1205.2688 [hep-ph]], M. R. Buckley and D. Hooper, Phys. Rev. D **86**, 043524 (2012) [arXiv:1205.6811 [hep-ph]].

[5] E. Dudas, Y. Mambrini, S. Pokorski and A. Romagnoni, JHEP **1210**, 123 (2012) [arXiv:1205.1520 [hep-ph]], K. -Y. Choi and O. Seto, Phys. Rev. D **86**, 043515 (2012) [Erratum-ibid. D **86**, 089904 (2012)] [arXiv:1205.3276 [hep-ph]], B. Kyae and J. -C. Park, arXiv:1205.4151 [hep-ph], H. M. Lee, M. Park and W. -I. Park, Phys. Rev. D **86**, 103502 (2012) [arXiv:1205.4675 [hep-ph]], D. Das, U. Ellwanger and P. Mitropoulos, JCAP **1208**, 003 (2012) [arXiv:1206.2639 [hep-ph]], Z. Kang, T. Li, J. Li and Y. Liu, arXiv:1206.2863 [hep-ph], J. -C. Park and S. C. Park, Phys. Lett. B **718**, 1401 (2013) [arXiv:1207.4981 [hep-ph]], Y. Bai and J. Shelton, JHEP **1212**, 056 (2012) [arXiv:1208.4100 [hep-ph]], L. Wang and X. -F. Han, Phys. Rev. D **87**, 015015 (2013) [arXiv:1209.0376 [hep-ph]], K. Schmidt-Hoberg, F. Staub and M. W. Winkler, JHEP **1301**, 124 (2013) [arXiv:1211.2835 [hep-ph]], G. Chalons, M. J. Dolan and C. McCabe, arXiv:1211.5154 [hep-ph].

[6] W. Buchmuller and M. Garny, JCAP **1208**, 035 (2012) [arXiv:1206.7056 [hep-ph]].

[7] N. Jarosik, C. L. Bennett, J. Dunkley, B. Gold, M. R. Greason, M. Halpern, R. S. Hill and G. Hinshaw *et al.*, Astrophys. J. Suppl. **192**, 14 (2011) [arXiv:1001.4744 [astro-ph.CO]].

[8] V. Silveira and A. Zee, Phys. Lett. B **161**, 136 (1985), J. McDonald, Phys. Rev. D **50**, 3637 (1994) [hep-ph/0702143 [HEP-PH]], C. P. Burgess, M. Pospelov and T. ter Veldhuis, M. C. Bento, O. Bertolami, R. Rosenfeld and L. Teodoro, Phys. Rev. D **62**, 041302 (2000) [astro-ph/0003350], Nucl. Phys. B **619**, 709 (2001) [hep-ph/0011335], V. Barger, P. Langacker, M. McCaskey, M. J. Ramsey-Musolf and G. Shaughnessy, Phys. Rev. D **77**, 035005 (2008) [arXiv:0706.4311 [hep-ph]], S. Andreas, T. Hambye and M. H. G. Tytgat, JCAP **0810**, 034 (2008) [arXiv:0808.0255 [hep-ph]], C. E. Yaguna, JCAP **0903**, 003 (2009) [arXiv:0810.4267 [hep-ph]], X. -G. He, T. Li, X. -Q. Li, J. Tandean and H. -C. Tsai,

Phys. Rev. D **79**, 023521 (2009) [arXiv:0811.0658 [hep-ph]], X. -G. He, T. Li, X. -Q. Li, J. Tandean and H. -C. Tsai, Phys. Lett. B **688**, 332 (2010) [arXiv:0912.4722 [hep-ph]], A. Bandyopadhyay, S. Chakraborty, A. Ghosal and D. Majumdar, JHEP **1011**, 065 (2010) [arXiv:1003.0809 [hep-ph]], S. Andreas, C. Arina, T. Hambye, F. -S. Ling and M. H. G. Tytgat, Phys. Rev. D **82**, 043522 (2010) [arXiv:1003.2595 [hep-ph]], Y. Mambrini, Phys. Rev. D **84**, 115017 (2011) [arXiv:1108.0671 [hep-ph]].

[9] S. Profumo, L. Ubaldi and C. Wainwright, Phys. Rev. D **82**, 123514 (2010) [arXiv:1009.5377 [hep-ph]].

[10] A. Biswas and D. Majumdar, arXiv:1102.3024 [hep-ph].

[11] S. Chatrchyan *et al.* [CMS Collaboration], Phys. Lett. B **716**, 30 (2012) [arXiv:1207.7235 [hep-ex]], G. Aad *et al.* [ATLAS Collaboration], Phys. Lett. B **716**, 1 (2012) [arXiv:1207.7214 [hep-ex]].

[12] E. Ma, Phys. Rev. D **73**, 077301 (2006) [hep-ph/0601225], L. Lopez Honorez, E. Nezri, J. F. Oliver and M. H. G. Tytgat, JCAP **0702**, 028 (2007) [hep-ph/0612275], D. Majumdar and A. Ghosal, Mod. Phys. Lett. A **23**, 2011 (2008) [hep-ph/0607067], M. Gustafsson, E. Lundstrom, L. Bergstrom and J. Edsjo, Phys. Rev. Lett. **99**, 041301 (2007) [astro-ph/0703512 [ASTRO-PH]], Q. -H. Cao, E. Ma and G. Rajasekaran, Phys. Rev. D **76**, 095011 (2007) [arXiv:0708.2939 [hep-ph]], E. Lundstrom, M. Gustafsson and J. Edsjo, Phys. Rev. D **79**, 035013 (2009) [arXiv:0810.3924 [hep-ph]], E. Nezri, M. H. G. Tytgat and G. Vertongen, JCAP **0904**, 014 (2009) [arXiv:0901.2556 [hep-ph]], S. Andreas, M. H. G. Tytgat and Q. Swillens, JCAP **0904**, 004 (2009) [arXiv:0901.1750 [hep-ph]], C. Arina, F. -S. Ling and M. H. G. Tytgat, JCAP **0910**, 018 (2009) [arXiv:0907.0430 [hep-ph]], L. Lopez Honorez and C. E. Yaguna, JHEP **1009**, 046 (2010) [arXiv:1003.3125 [hep-ph]], D. Borah and J. M. Cline, Phys. Rev. D **86**, 055001 (2012) [arXiv:1204.4722 [hep-ph]].

[13] L. Lopez Honorez and C. E. Yaguna, JCAP **1101**, 002 (2011) [arXiv:1011.1411 [hep-ph]].

[14] R. Barbieri, L. J. Hall and V. S. Rychkov, Phys. Rev. D **74**, 015007 (2006) [hep-ph/0603188].

[15] M. Kadastik, K. Kannike and M. Raidal, Phys. Rev. D **81**, 015002 (2010) [arXiv:0903.2475 [hep-ph]], M. Kadastik, K. Kannike and M. Raidal, Phys. Rev. D **80**, 085020 (2009) [Erratum-ibid. D **81**, 029903 (2010)] [arXiv:0907.1894 [hep-ph]].

[16] Q. -H. Cao, E. Ma, J. Wudka and C. -P. Yuan, arXiv:0711.3881 [hep-ph].

[17] J. F. Navarro, C. S. Frenk and S. D. M. White, Astrophys. J. **490**, 493 (1997) [astro-ph/9611107].

[18] J. Einasto, Trudy Inst. Astrofiz. Alma-Ata **5** (1965) 87, J. F. Navarro *et al.*, Mon. Not. Roy. Astron. Soc. **349**, 1039 (2004); astro-ph/0311231.

[19] G. Abbiendi *et al.* [OPAL Collaboration], Eur. Phys. J. C **19**, 587 (2001) [hep-ex/0012018].

[20] R. Barbieri, M. Frigeni and G. F. Giudice, Nucl. Phys. B **313**, 725 (1989).

[21] A. Melfo, M. Nemevsek, F. Nesti, G. Senjanovic and Y. Zhang, Phys. Rev. D **84** (2011) 034009 [arXiv:1105.4611 [hep-ph]].

[22] Y. Mambrini, Phys. Rev. D **84** (2011) 115017 [arXiv:1108.0671 [hep-ph]], J. Giedt, A. W. Thomas and R. D. Young, Phys. Rev. Lett. **103** (2009) 201802 [arXiv:0907.4177 [hep-ph]].

[23] E. Aprile *et al.* [XENON100 Collaboration], Phys. Rev. Lett. **109**, 181301 (2012) [arXiv:1207.5988 [astro-ph.CO]].

[24] E. Aprile *et al.* [XENON100 Collaboration], Phys. Rev. Lett. **107**, 131302 (2011) [arXiv:1104.2549 [astro-ph.CO]].

[25] Z. Ahmed *et al.* [CDMS-II Collaboration], Science **327**, 1619 (2010) [arXiv:0912.3592 [astro-ph.CO]].

[26] E. Armengaud *et al.* [EDELWEISS Collaboration], Phys. Lett. B **702**, 329 (2011) [arXiv:1103.4070 [astro-ph.CO]].

[27] G. Belanger and J. -C. Park, JCAP **1203**, 038 (2012) [arXiv:1112.4491 [hep-ph]].

[28] J. Edsjo and P. Gondolo, Phys. Rev. D **56**, 1879 (1997) [hep-ph/9704361].

[29] W-L. Guo and Y-L. Wu, JHEP **1010** (2010) 083 [arXiv:1006.2518 [hep-ph]].

[30] G. Abbiendi *et al.* [ALEPH and DELPHI and L3 and OPAL and The LEP working group for Higgs boson searches Collaborations], [arXiv:1301.6065 [hep-ex]].

[31] M. Cirelli, G. Corcella, A. Hektor, G. Hutsi, M. Kadastik, P. Panci, M. Raidal and F. Sala *et al.*, JCAP **1103**, 051 (2011) [Erratum-ibid. **1210**, E01 (2012)] [arXiv:1012.4515 [hep-ph]].

[32] R. Catena and P. Ullio, JCAP **1008**, 004 (2010) [arXiv:0907.0018 [astro-ph.CO]], P. Salucci, F. Nesti, G. Gentile and C. F. Martins, Astron. Astrophys. **523**, A83 (2010) [arXiv:1003.3101 [astro-ph.GA]].

[33] M. Ackermann *et al.* [LAT Collaboration], Phys. Rev. D **86**, 022002 (2012) [arXiv:1205.2739 [astro-ph.HE]].